Asymptotic stability and chaotic motions in trajectory following feedback controlled robots

B. Sandeep Reddy
Graduate Student,
Department of Mechanical Engineering,
Indian Institute of Science,
Bangalore-560012, India
Email: bsandeep@mecheng.iisc.ernet.in

Ashitava Ghosal*

Professor, Department of
Department of Mechanical Engineering,
Indian Institute of Science,
Bangalore-560012, India
Email: asitava@mecheng.iisc.ernet.in

A feedback controlled robot manipulator with positive controller gains is known to be asymptotically stable at a set point and for trajectory following in the sense of Lyapunov. However, when the end-effector of a robot or its joints are made to follow a time dependent trajectory, the nonlinear dynamical equations modeling the feedback controlled robot can also exhibit chaotic motions and as a result cannot follow a desired trajectory. In this paper, using the example of a simple two-degree-of-freedom robot with two rotary (R) joints, we take a re-look at the asymptotic stability of a 2R robot following a desired time dependent trajectory under a proportional plus derivative (PD) and a model-based computed torque control. We demonstrate that the condition of positive controller gains is not enough and the gains must be large for chaos not to occur and for the robot to asymptotically follow a desired trajectory. We apply the method of multiple scales to the two nonlinear second-order ordinary differential equations which describes the dynamics of the feedback controlled 2R robot and derive a set of four first-order slow flow equations. At a fixed point, the Routh-Hurwitz criterion is used to obtain values of proportional and derivative gains at which the controller is asymptotically stable or indeterminate. For the model-based control, a parameter representing model mismatch is used and the controller gains for a chosen mismatch parameter value are obtained. From numerical simulations with controller gain values in the indeterminate region, its is shown that for some values, the nonlinear dynamical equations are chaotic and hence the 2R robot cannot follow the desired trajectory and be asymptotically stable.

Keywords: Asymptotic stability, Trajectory following, Planar 2R robot, Chaotic motion, Multiple scales analysis

1 Introduction

The stability of dynamical systems is an important area of study in nonlinear dynamics. A stable system is one which for a bounded input, the output or the trajectories of the system stay in bounded neighborhood of the equilibrium point. A system is said to be asymptotically stable if in addition to being stable, the trajectories approach the equilibrium point as time tends to infinity [1]. In a robot following a desired trajectory with a prescribed tolerance, simple stability is not enough and the robot controller must ensure asymptotic stability. In the field of robotics, extensive research has been done to design and implement controllers and asymptotic stability of controllers has been demonstrated by numerical simulation. References [2, 3] demonstrate asymptotic stability of robot manipulators using PID control, whereas reference [4] demonstrates asymptotic stability for a robot manipulator based on PD control. Asymptotic stability has also been shown for planar multi-link flexible manipulators [5] and for a robot manipulator using adaptive fuzzy control [6]. Asymptotic stability has also been demonstrated experimentally for PID control of robot manipulators [7, 8], PD control of closed chain mechanical systems [9] and Lyapunov-based control of robot and mass-spring system undergoing an impact collision [10]. It has also been shown theoretically, using Lyapunov stability, that a robot is asymptotically stable when the desired velocity is zero (or set point control) [11] and for a trajectory with non-zero velocity and accelera-

*Address all correspondence to this author.

tion [12] when the controller gains are greater than zero. The nonlinear equations modeling a feedback controlled robot can, however, exhibit chaos. Chaos has been demonstrated in a double pendulum (see, for example, [13, 14]) and in a planar 2R robot (see, for example, [15–17]). In a chaotic system, the trajectories fill up the entire state space [18] without tracking the desired trajectory. In this paper, we study the nonlinear equations modeling a simple 2R planar robot, under feedback control following a desired trajectory and show that the condition of positive gains is not enough and the gains need to be large for asymptotic stability. We obtain values of controller gains for which the robot equations show asymptotic stability or chaos. We study two well-known controllers, namely a proportional plus derivative and a model-based computed torque controller.

In this paper, we propose a semi-analytical approach to derive the ranges of proportional and derivative gains for which the nonlinear dynamical equations modeling the feedback controlled 2R planar robot can be chaotic. The approach is based on the use of the method of multiple scales (MMS) [19] to obtain slow flow equations whose existence ensures a bounded solution of the nonlinear equations. The fixed points of the slow flow equations are obtained and the stability in the neighborhood of these fixed points is investigated using the Routh-Hurwitz criterion [20]. The Routh-Hurwitz criterion yields the values of controller gains for which the 2R robot is asymptotically stable or indeterminate. To resolve the indeterminacy, we resort to numerical simulations and show that for certain values of the controller gains, some of the indeterminate points result in chaos and hence the planar 2R robot is not asymptotically stable at these gain values. For the model-based computed torque controller, a parameter is used to quantify the mismatch in the estimate, and again MMS and Routh-Hurwitz criterion is used to obtain controller gain values for which the model-based computed torque controller results in asymptotic stability or indeterminacy. It is shown that chaotic behavior is observed for small derivative gains and large under-estimation of model parameters and chaos is not observed when the frequency of the desired trajectory is large. Since the indeterminacy is resolved using numerical computations, the approach presented in this paper is only partially analytical.

This paper is organized as follows: In section 2, we present the dynamic equations of motion of the feedback controlled robot. We present an approach to non-dimensionalize the nonlinear equations so as to reduce the number of parameters. In section 3, we present the method of multiple scales and its application to the planar 2R robot under proportional plus derivative (PD) and a model-based computed torque control, and derive the four slow flow equations. In section 4, we derive the conditions for asymptotic stability and indeterminacy using the Routh-Hurwitz criterion. In section 5, we present numerical results giving the ranges of controller gains for which the 2R robot is asymptotically stable. We resolve the points in the indeterminate region using numerical simulations of the slow flow equations, and by computing the Lyapunov exponents [21] we show that some of the controller gains in the indeterminate regions are chaotic. In section 6, we summarize the paper and present the main conclusions.

2 Mathematical Modeling of the 2R Planar Robot

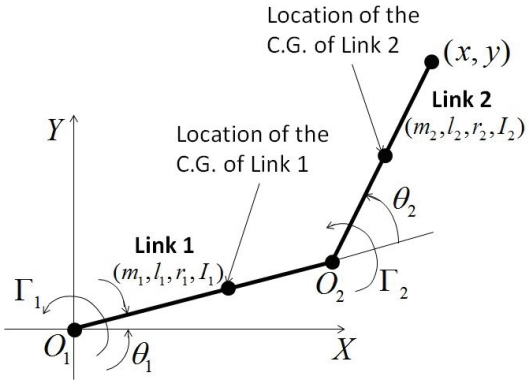

Fig. 1. A planar 2R robot

Fig. 1 shows the schematic of a two-degree-of-freedom robot consisting of two rotary (R) joints actuated by two DC servo motors which can generate torques Γ_1 and Γ_2 respectively. The tip of the robot, point (x,y) traces a trajectory in the horizontal plane as the R joints are rotated and the trajectory is a function of time. The equations of motion of the 2R planar robot are available in standard textbooks on robotics (see, for example, [22]) and are a set of two non-linear ordinary differential equations (ODEs) of the form

$$\begin{aligned}
&[I_1 + m_2(l_1^2 + r_2^2) + m_1 r_1^2 + 2m_2 l_1 r_2 \cos\theta_2]\ddot{\theta}_1 + [m_2 r_2^2 \\
&+ I_2 + m_2 l_1 r_2 \cos\theta_2]\ddot{\theta}_2 - m_2 l_1 r_2 \sin\theta_2 [2\dot{\theta}_1 + \dot{\theta}_2]\dot{\theta}_2 = \Gamma_1 \\
&[m_2 r_2^2 + I_2 + m_2 l_1 r_2 \cos\theta_2]\ddot{\theta}_1 + [m_2 r_2^2 + I_2]\ddot{\theta}_2 \\
&+ m_2 l_1 r_2 \sin\theta_2 \dot{\theta}_1^2 = \Gamma_2
\end{aligned} \tag{1}$$

where m_j, l_j, I_j, r_j $(j = 1,2)$ are the masses, lengths, inertia and position of center of mass of link j respectively, and (Γ_1, Γ_2) are the joint torques. To trace a desired trajectory, feedback control is used and a typical robot controller implementing a proportional plus derivative (PD) control scheme is given by

$$\Gamma_i = \ddot{\theta}_{d_i} + K_v \dot{e}_i + K_p e_i,\ i = 1,2 \tag{2}$$

where K_p and K_v are the controller gains, $e_i = \theta_{d_i} - \theta_i$ is the servo error, $\dot{e}_i$ is the derivative of the servo error and θ_{d_i} is the desired trajectory to be traced. The controller gains for the two motors can be different. However, in this work, as a simplifying assumption, they are assumed to be same.

The desired trajectory θ_{d_i}, $i = 1,2$ is assumed to be periodic and given by

$$\theta_{d_i} = A_{f_i} \sin(\Omega t),\ i = 1,2 \tag{3}$$

where A_{f_i} is the amplitude and Ω is the forcing frequency.

Another well-known control scheme uses the dynamic model of a robot and in this model-based control, the joint torques are computed as

$$\Gamma = [\alpha]\Gamma_p + \beta \tag{4}$$

where Γ_p is the servo portion of the control scheme as given by equation (2) and $[\alpha]$, β are determined from the dynamic model [22]. Typically the dynamic model is not known exactly and only estimates of the mass, inertia and other geometric parameters are known. The estimated mass and other parameters are assumed to be of the form

$$\begin{aligned} &\hat{m}_i = (1+e)m_i,\ \hat{r}_i = (1+e)r_i, \\ &\hat{I}_i = (1+e)I_i,\quad \hat{l}_i = (1+e)l_i,\ i = 1,2 \end{aligned} \tag{5}$$

where $e > 0$ implies an overestimated model and $e < 0$ implies an underestimated model. Since the mass cannot be negative, $-1 < e < \infty$.

The number of parameters in the above equations can be reduced by non-dimensionalization as follows:

We define the non-dimensional time τ as Ωt, and get

$$\begin{aligned} \frac{d\theta_j}{dt} &= \frac{d\theta_j}{d\tau}.\frac{d\tau}{dt} = \Omega\frac{d\theta_j}{d\tau} = \Omega\theta_j' \\ \frac{d^2\theta_j}{dt^2} &= \Omega^2\frac{d^2\theta_j}{d\tau^2} = \Omega^2\theta_j'' \end{aligned} \tag{6}$$

where "$\prime$" represents derivative with respect to τ.

Next we introduce the non-dimensional variables [23]

$$P_1 = \frac{m_1 r_1^2 + I_1}{m_2 r_2^2 + I_2},\ P_2 = \frac{m_2 l_1^2}{m_2 r_2^2 + I_2},\ P_3 = \frac{r_2}{l_1} \tag{7}$$

Using equations (6) and (7) in equation (1) and dividing both sides of equation (1) by $(m_2 r_2^2 + I_2)$, the non-dimensionalized equations of motion of a 2R planar robot are given by

$$\begin{aligned} &[P_1 + 1 + P_2 + 2P_2P_3\cos(\theta_2)]\theta_1'' + [1 + P_2P_3\cos(\theta_2)]\theta_2'' \\ &- P_2P_3\sin(\theta_2)[2\theta_1' + \theta_2']\theta_2' = \Gamma_{1n} \\ &[1 + P_2P_3\cos(\theta_2)]\theta_1'' + \theta_2'' + P_2P_3\sin(\theta_2)\theta_1'^2 = \Gamma_{2n} \end{aligned} \tag{8}$$

where Γ_{1n}, Γ_{2n} are the non-dimensional torques whose expressions depend on the controller.

PD control of a planar 2R robot

For a PD control, the non-dimensional torques are

$$\Gamma_{in} = S_n\theta_{d_i}'' + K_{vn}e_i' + K_{pn}e_i,\ i = 1,2 \tag{9}$$

where $S_n = 1/(m_2 r_2^2 + I_2)$, $K_{pn} = K_p/\Omega^2(m_2 r_2^2 + I_2)$, $K_{vn} = K_v/\Omega(m_2 r_2^2 + I_2)$ and θ_{d_i} and its derivatives can be derived from equations (3) and (6).

Model-based control of a planar 2R robot

To non-dimensionalize the equations, we use three non-dimensional parameters in addition to those defined in equation (7) as

$$\begin{aligned} &\alpha_1 = \frac{\hat{m}_1\hat{r}_1^2 + \hat{I}_1 + \hat{m}_2\hat{r}_2^2 + \hat{I}_2 + \hat{m}_2\hat{l}_1^2}{m_2 r_2^2 + I_2},\ \alpha_2 = \frac{\hat{m}_2\hat{l}_1\hat{r}_2}{m_2 r_2^2 + I_2} \\ &\alpha_3 = \frac{\hat{m}_2\hat{r}_2^2 + \hat{I}_2}{m_2 r_2^2 + I_2} \end{aligned} \tag{10}$$

Using the above non-dimensional parameters, Γ_{1n} and Γ_{2n} can be obtained in a similar manner as in the PD control and the non-dimensional feedback control equations of the 2R robot can be written as

$$\begin{aligned} &\begin{bmatrix} P_1 + 1 + P_2 + 2P_2P_3\cos(\theta_2) & 1 + P_2P_3\cos(\theta_2) \\ 1 + P_2P_3\cos(\theta_2) & 1 \end{bmatrix} \begin{bmatrix} \theta_1'' \\ \theta_2'' \end{bmatrix} \\ &+ \begin{bmatrix} -P_2P_3\sin(\theta_2)[2\theta_1' + \theta_2']\theta_2' \\ P_2P_3\sin(\theta_2)\theta_1'^2 \end{bmatrix} = \\ &\begin{bmatrix} \alpha_1(\theta_{d_1}'' + K_{pn}(\theta_{d_1} - \theta_1) + K_{vn}(\theta_{d_1}' - \theta_1')) \\ +\alpha_3(\theta_{d_2}'' + K_{pn}(\theta_{d_2} - \theta_2) + K_{vn}(\theta_{d_2}' - \theta_2')) \\ +\alpha_2(\cos(\theta_2)(2\theta_{d_1}'' + \theta_{d_2}'' + K_{pn}(2\theta_{d_1} - 2\theta_1 + \theta_{d_2} - \theta_2) \\ +K_{vn}(2\theta_{d_1}' - 2\theta_1' + \theta_{d_2}' - \theta_2')) - \sin(\theta_2)[2\theta_1' + \theta_2']\theta_2') \\ \\ \alpha_2(\cos(\theta_2)(\theta_{d_1}'' + K_{pn}(\theta_{d_1} - \theta_1) + \\ K_{vn}(\theta_{d_1}' - \theta_1')) + \theta_2\theta_1'^2) + \alpha_3(\theta_{d_1}'' + \theta_{d_2}'' + K_{pn}(\theta_{d_1} \\ -\theta_1 + \theta_{d_2} - \theta_2) + K_{vn}(\theta_{d_1}' - \theta_1' + \theta_{d_2}' - \theta_2')) \end{bmatrix} \end{aligned} \tag{11}$$

where $K_{pn} = K_p/\Omega^2$ and $K_{vn} = K_v/\Omega$.

The PD and model-based control were studied in reference [15, 16] and, using numerical search, values of controller gains K_p, K_v and e were obtained for which the robot control equations demonstrated chaos and hence *not* asymptotically stable. In section 4 we present a semi-analytical approach to obtain the ranges of K_p, K_v and e for which the trajectory following planar 2R robot is asymptotically stable.

3 The Method of Multiple Scales

The method of multiple scales (MMS) is a well-known singular perturbation method which examines the behavior of a nonlinear system of equations at various time scales to obtain insight into the behavior of a nonlinear dynamical system. There are several examples of analysis of nonlinear systems using MMS (see, for example, [24–27]). In this section, we apply the method of multiple scales to the PD and model based feedback control equations. We seek a uniform expansion for the solution of the above equations in the form

$$\theta_1 = \sum_{i=0}^{2}\varepsilon^{i+1}\theta_{1i}(T_0, T_1, T_2),\quad \theta_2 = \sum_{i=0}^{2}\varepsilon^{i+1}\theta_{2i}(T_0, T_1, T_2) \tag{12}$$

where, ε is a small dimensionless measure of the variables θ_1, θ_2. The variable T_0 (same as τ) is the fast scale associated with changes occurring at the forcing frequencies Ω and the natural frequencies ω_n, and $T_1 = \varepsilon\tau$ and $T_2 = \varepsilon^2\tau$ are the slow scales associated with the modulations of the amplitudes and phases due to non-linearities. Also, the derivatives are treated as

$$\begin{aligned}\frac{d}{dt} &= D_0 + \varepsilon D_1 + \varepsilon^2 D_2 + ..\\ \frac{d^2}{dt^2} &= D_0^2 + \varepsilon(2D_0D_1) + \varepsilon^2(2D_0D_2 + D_1^2) + ..\end{aligned} \tag{13}$$

First we apply MMS to the PD controller and then to the model-based controller.

Application of MMS to PD control

Before we apply MMS, we must resolve two problems. First, an examination of the equation describing feedback control of the 2R robot, reveals the presence of trigonometric functions in the form of $\cos(\theta_2)$ and $\sin(\theta_2)$. It is not possible to apply MMS to sine and cosine terms, as MMS requires the computation of natural frequencies at the first order and trigonometric terms are not linearly reducible. To resolve this, keeping in mind that the 2R robot equations given by equation (1) have only one fixed point $(0,0,0,0)$, we resort to an expansion in Taylor series around the fixed point. We expand these trigonometric terms as

$$\cos(\theta_2) = 1 - (\theta_2^2/2!),\ \sin(\theta_2) = \theta_2 - (\theta_2^3/3!) \approx \theta_2 \tag{14}$$

The expansion given in equation (14) represents the common way available in literature to deal with trigonometric terms [28, 29]. It is also appropriate to neglect the cubic term for the expansion of $\sin(\theta_2)$ since the highest order of expansion according to equation (12) is three. An examination of use of $\sin(\theta_2)$ in equation of motion reveals that it is coupled with a quadratic term. When the expansion given by equation (12) is done, $\sin(\theta_2)$ coupled with the quadratic term gives a cubic term (order three). If the cubic term in equation (14) had been also considered, then coupled with the quadratic term would have given a fifth-order term – higher than highest order of expansion we consider in equation (12).

Secondly, we need to consider how the terms have to be ordered according to various time scales. We order the inertial terms, stiffness terms (K_p) and the forcing terms ($A_{f_i}\sin(\tau)$) at time scale $T_0 = \tau$, i.e., at the faster time scale. We order the dissipative terms (K_v) at time scale $T_2 = \varepsilon^2\tau$ which is the slower time scale. The non-linearities due to the cubic terms in the equations automatically appear at time scale T_2. Lastly, the control equations also has the terms $\sin(\tau)$ and $\cos(\tau)$. We rewrite them as $\sin(\tau) = (1/2i)(e^{i\tau} - e^{-i\tau})$ and $\cos(\tau) = (1/2)(e^{i\tau} + e^{-i\tau})$.

The equations of motion of the planar 2R robot driven by PD control with the ordering and other modifications described above can be written as

$$\begin{aligned}&[P_1 + 1 + P_2 + 2P_2P_3\left(1 - \frac{\theta_2^2}{2}\right)]\theta_1'' + [1 + P_2P_3\\ &\left(1 - \frac{\theta_2^2}{2}\right)]\theta_2'' - P_2P_3\theta_2[2\theta_1' + \theta_2']\theta_2' = -K_{pn}\theta_1\\ &-\varepsilon^2K_{vn}\theta_1' + \varepsilon A_{f_1}((iE_1 + E_2)e^{i\tau} + (-iE_1 + E_2)e^{-i\tau})\\ &[1 + P_2P_3\left(1 - \frac{\theta_2^2}{2}\right)]\theta_1'' + \theta_2'' + P_2P_3\theta_2\theta_1'^2 = -K_{pn}\theta_2\\ &-\varepsilon^2K_{vn}\theta_2' + \varepsilon A_{f_2}((iE_1 + E_2)e^{i\tau} + (-iE_1 + E_2)e^{-i\tau})\end{aligned} \tag{15}$$

where $E_1 = (S_n - K_{pn})/2$ and $E_2 = (K_{vn}/2)$.

Using equation (13) in equation (15) and equating coefficients of like powers of ε, we obtain

Order ε

$$\begin{aligned}&(P_1 + 1 + P_2 + 2P_2P_3)D_0^2\theta_{10} + (1 + P_2P_3)D_0^2\theta_{20} +\\ &K_{pn}\theta_{10} = A_{f_1}((iE_1 + E_2)e^{i\tau} + (-iE_1 + E_2)e^{-i\tau})\\ &(1 + P_2P_3)D_0^2\theta_{10} + D_0^2\theta_{20} + K_{pn}\theta_{20} =\\ &A_{f_2}((iE_1 + E_2)e^{i\tau} + (-iE_1 + E_2)e^{-i\tau})\end{aligned} \tag{16}$$

where $D_n^2 = (\partial^2/\partial T_n^2)$. The solution of equation (16) is of the form

$$\begin{aligned}&\theta_{10} = A_1e^{i\omega_1T_0} + A_2e^{i\omega_2T_0} + F_1(E_{w1}e^{iT_0} + E_{w2}e^{-iT_0})\\ &+ c.c.,\ \ \theta_{20} = c_{21}A_1e^{i\omega_1T_0} + c_{22}A_2e^{i\omega_2T_0}\\ &+ F_2(E_{w1}e^{iT_0} + E_{w2}e^{-iT_0}) + c.c.\end{aligned} \tag{17}$$

where $E_{w1} = iE_1 + E_2$ and $E_{w2} = -iE_1 + E_2$, ω_1 and ω_2 are the natural frequencies of the system, $c.c$ stands for complex conjugate and the terms in equation (17) is given in the Appendix. The above equation is used in computing terms at order ε^2 and ε^3 shown next.

Order ε^2

$$\begin{aligned}&(P_1 + 1 + P_2(1 + 2P_3))D_0^2\theta_{11} + (1 + P_2P_3)D_0^2\theta_{21}\\ &+ K_{pn}\theta_{11} = -2(P_1 + 1 + P_2(1 + 2P_3))D_0D_1\theta_{10}\\ &- 2(1 + P_2P_3)D_0D_1\theta_{20}\\ &(1 + P_2P_3)D_0^2\theta_{11} + D_0^2\theta_{21} + K_{pn}\theta_{21} =\\ &- 2(1 + P_2P_3)D_0D_1\theta_{10} - 2D_0D_1\theta_{20}\end{aligned} \tag{18}$$

In the above equation on the right-hand side, the non-secular terms are zero. Equating the secular terms on the right-hand side to zero would give $A_1(T_1)$ and $A_2(T_1)$. Hence, substituting equation (17) into the right-hand side of equation (18) and equating the secular terms to zero, we get

$$\begin{aligned}&-2(P_1 + 1 + P_2 + 2P_2P_3)\frac{\partial A_1}{\partial T_1} - 2(1 + P_2P_3)\frac{\partial A_2}{\partial T_1} = 0\\ &-2(1 + P_2P_3)\frac{\partial A_1}{\partial T_1} - 2\frac{\partial A_2}{\partial T_1} = 0\end{aligned} \tag{19}$$

Solving equation (19), we get

$$\partial A_1/\partial T_1 = 0,\ \partial A_2/\partial T_1 = 0 \tag{20}$$

From equation (20), we have A_1=$A_1(T_0,T_2)$ and A_2=$A_2(T_0,T_2)$. Now at order ε^3, we have

Order ε^3

$$\begin{aligned}
&(P_1+1+P_2(1+2P_3))D_0^2\theta_{12}+(1+P_2P_3)D_0^2\theta_{22}\\
&+K_{pn}\theta_{12}=P_2P_3(\theta_{20}^2\left(D_0^2\theta_{10}+(1/2)D_0^2\theta_{20}\right)\\
&+\theta_{20}(2D_0\theta_{10}+D_0\theta_{20})D_0\theta_{20})-K_{vn}D_0\theta_{10}\\
&(1+P_2P_3)D_0^2\theta_{12}+D_0^2\theta_{22}+K_{pn}\theta_{22}=\\
&P_2P_3(D_0^2\theta_{10}(1/2)\theta_{20}^2-\theta_{20}(D_0\theta_{10})^2)-K_{vn}D_0\theta_{20}
\end{aligned} \tag{21}$$

Equation (21) represents the third-order approximation for the 2R planar robot system. Now, we must separate the secular terms in equation (21), to determine the solvability conditions (or the slow flow equations). We do this by introducing a detuning parameterσ_1 [19] related to Ω as

$$3\Omega=\omega_1+3\varepsilon\sigma_1,\ \ \Omega=(1/2)(\omega_1-\omega_2)+\varepsilon\sigma_1 \tag{22}$$

To determine the solvability conditions, we seek a particular solution free of secular terms corresponding to the terms proportional to $e^{i\omega_n T_0}$, in the form

$$\theta_{12}=\sum_{i=1}^{2}G_i(T_1)e^{i\omega_i T_0},\ \ \theta_{22}=\sum_{i=1}^{2}H_i(T_1)e^{i\omega_i T_0} \tag{23}$$

Substituting equation (17) and equation (22) into the right-hand side of equation (21) and substituting equation (23) into the left-hand side of equation (21), and equating the coefficients of the powers of $e^{i\omega_1 T_0}$ and $e^{i\omega_2 T_0}$, we can determine the solvability conditions, thus eliminating the secular terms [19]. Considering, after the above mentioned substitution into equation (21) at powers $e^{i\omega_1 T_0}$ and $e^{i\omega_2 T_0}$, we get

At $e^{i\omega_1 T_0}$

$$\begin{aligned}
&A_1^{'}=A_1(-J_{121}+i(J_{122}+J_{123}A_1^2+J_{124}A_2^2))+\\
&A_2(-J_{131}+iJ_{132})e^{2i\sigma_1 T_1}+iJ_{14}(iE_1+E2)^3e^{3i\sigma_1 T_1}
\end{aligned} \tag{24}$$

At $e^{i\omega_2 T_0}$

$$\begin{aligned}
&A_2^{'}=A_2(-J_{221}+i(J_{222}+J_{223}A_1^2+J_{224}A_2^2))+\\
&A_1(-J_{231}+iJ_{232})e^{-2i\sigma_1 T_1}
\end{aligned} \tag{25}$$

where the terms $L_{11},J_{121},L_{21},J_{221},...$ are given in the Appendix. Introducing the polar notation $A_n=a_n e^{ib_n}$ and using in equations (24-25), we get

$$\begin{aligned}
&a_1^{'}=-J_{121}a_1+a_2(-J_{131}\cos\gamma-J_{132}\sin\gamma)-J_{151}\cos\delta\\
&-J_{152}\sin\delta,\quad b_1^{'}=J_{122}+J_{123}a_1^2+J_{124}a_2^2+\\
&\frac{a_2(-J_{131}\sin\gamma+J_{132}\cos\gamma)}{a_1}+\frac{-J_{151}\sin\delta+J_{152}\cos\delta}{a_1}\\
&a_2^{'}=-J_{221}a_1+a_1(-J_{231}\cos\gamma+J_{232}\sin\gamma)\\
&b_2^{'}=J_{222}+J_{223}a_1^2+J_{224}a_2^2+\frac{a_1(J_{231}\sin\gamma+J_{332}\cos\gamma)}{a_2}
\end{aligned} \tag{26}$$

where $\delta=3\sigma_1T_1-b_1$ and $\gamma=2\sigma_1T_1+b_2-b_1$. Modifying coordinates, using $x=a_1\cos\delta$, $y=a_1\sin\delta$, $z=a_2\cos(\delta-\gamma)$ and $w=a_2\sin(\delta-\gamma)$, we have the final set of four slow flow equations given by

$$\begin{aligned}
&x'=-J_{121}x-(3\sigma_1-J_{122})y+y(J_{123}(x^2+y^2)+\\
&J_{124}(z^2+w^2))+J_{13}(-2E_1E_2z+(E_2^2-E_1^2)w)\\
&-J_{14}E_1(3E_2^2-E_1^2)\\
&y'=-J_{121}y+(3\sigma_1-J_{122})x-x(J_{123}(x^2+y^2)\\
&+J_{124}(z^2+w^2))+J_{13}(-2E_1E_2w-(E_2^2-E_1^2)z)\\
&-J_{14}E_2(E_2^2-3E_1^2)\\
&z'=-J_{221}z-(\sigma_1-J_{222})w+w(J_{223}(x^2+y^2)+\\
&J_{224}(z^2+w^2))+J_{23}(2E_1E_2x+(E_2^2-E_1^2)y)\\
&w'=-J_{221}w+(\sigma_1-J_{222})z-z(J_{223}(x^2+y^2)+\\
&J_{224}(z^2+w^2))+J_{23}(2E_1E_2y-(E_2^2-E_1^2)x)
\end{aligned} \tag{27}$$

Equations (27) represent the slow flow equations and are the solvability conditions for the feedback control equations to have a bounded solution.

Application of MMS to model-based control

We now apply MMS to the equations of the 2R robot driven by the model-based computed torque control as given by equation (11). We order the terms in the case for PD control. After following the same procedure as in the case of PD control (from equation (16) onwards), the slow flow equations are obtained as

$$\begin{aligned}
&x'=-J_{121}x-(3\sigma_1-J_{122})y+y(J_{123}(x^2+y^2)\\
&+J_{124}(z^2+w^2))-J_{a1}z+J_{a2}w-J_{a3}\\
&y'=-J_{121}y+(3\sigma_1-J_{122})x-x(J_{123}(x^2+y^2)\\
&+J_{124}(z^2+w^2))-J_{a1}w-J_{a2}z-J_{a4}\\
&z'=-J_{221}z-(\sigma_1-J_{222})w+w(J_{223}(x^2+y^2)\\
&+J_{224}(z^2+w^2))-J_{a5}x+J_{a6}y\\
&w'=-J_{221}w+(\sigma_1-J_{222})z-z(J_{223}(x^2+y^2)\\
&+J_{224}(z^2+w^2))-J_{a5}y-J_{a6}x
\end{aligned} \tag{28}$$

where σ_1 is the detuning parameter of the same form (although numerically different) as given by equation (22) for

PD control. The terms $J_{121}, J_{122}, ...$ are different from those in the slow flow equations for PD control (equation (27)) and are given in the Appendix.

4 Asymptotic Stability Analysis

In this section, we derive the analytical conditions for the asymptotic stability for the system given by equations (27), (28) for the PD and model-based controllers respectively, at the fixed point of the both the systems. Equations (27), (28) are autonomous systems having nine fixed points. Although these fixed points cannot be explicitly given, we can compute them numerically. We discuss the stability of these systems at one of those fixed points, say $f_s = (x_s, y_s, z_s, w_s) - f$ is different for equations (27) and (28). To analyze the asymptotic stability of equation (27), (28), we use the Routh-Hurwitz criterion [30, 31], the central idea of which is that in order for any system of equations to be asymptotically stable, all eigenvalues of it's Jacobian must have negative real parts. We apply the Routh-Hurwitz criterion by following the sequence of steps:

STEP 1 - Compute the Jacobian of equations (27), (28) at fixed point f_s

$$J_f = \frac{\partial \mathbf{f}}{\partial \eta} \tag{29}$$

where $\mathbf{f} = (f_1, f_2, f_3, f_4)^T$ and $\eta = (x, y, z, w)^T$

STEP 2 - Compute the characteristic equation of the Jacobian J_f as

$$F_c = |J_f - \lambda I| = 0 \tag{30}$$

where I is 4×4 identity matrix. The characteristic equation of (30) is of the form

$$F_c = a_4\lambda^4 + a_3\lambda^3 + a_2\lambda^2 + a_1\lambda + a_0 \tag{31}$$

To apply the Routh-Hurwitz criterion, we write the Hurwitz matrix [30] which for the above fourth-order system is given by

$$\begin{bmatrix} a_3 & a_4 & 0 & 0 \\ a_1 & a_2 & a_3 & a_4 \\ 0 & a_0 & a_1 & a_2 \\ 0 & 0 & 0 & a_0 \end{bmatrix} \tag{32}$$

The principal diagonal minors Δ_i $i = 1, .., 4$ of the Hurwitz matrix are

$$\Delta_1 = a_3, \Delta_2 = \begin{bmatrix} a_3 & a_4 \\ a_1 & a_2 \end{bmatrix}, \Delta_3 = \begin{bmatrix} a_3 & a_4 & 0 \\ a_1 & a_2 & a_3 \\ 0 & a_0 & a_1 \end{bmatrix}, \Delta_4 = a_0\Delta_3 \tag{33}$$

From the Routh-Hurwitz criterion, the conditions for asymptotic stability require that all of the principal diagonal minors Δ_i to be positive provided $a_4 > 0$ [30, 31], i.e., we need

$$\begin{aligned} &a_4 > 0,\ \Delta_1 = a_3 > 0,\ \Delta_2 = a_2a_3 - a_4a_1 > 0 \\ &\Delta_3 = a_1a_2a_3 - a_4a_1^2 - a_3^2a_0 > 0,\ \Delta_4 = a_0 > 0 \end{aligned} \tag{34}$$

Simplifying the inequalities, the local asymptotic stability of the system at the fixed point f_s is guaranteed iff

$$\begin{aligned} &h_1 = a_i > 0 \ \ \forall i = 0, .., 4, \ \ h_2 = a_2a_3 - a_4a_1 > 0, \\ &h_3 = a_1a_2a_3 - a_4a_1^2 - a_3^2a_0 > 0 \end{aligned} \tag{35}$$

We can make the following comments from (35):

If all of $h_1, h_2, h_3 > 0$, then the system is **asymptotically stable** – all roots of the characteristic polynomial in equation (31) lie in the left half plane.

If any of $h_1, h_2, h_3 < 0$, then the system is **unstable** and at least one root of the polynomial in (31) lies in the right half plane. This case is not considered as the feedback controlled planar 2R robot is known to have simple stability for trajectory following [11].

If Δ_1, Δ_2, Δ_3 are positive, but $\Delta_4 = 0$, then the system is at the boundary of stability. Since $\Delta_4 = a_0\Delta_3$, then either $a_0 = 0$ or $\Delta_3 = 0$. If $a_0 = 0$, then one of the roots of the characteristic equation is zero and the system is on the *boundary* of aperiodic stability. If $\Delta_3 = 0$, then the system has two complex conjugate imaginary roots and the system is on the *boundary* of oscillatory stability [20]. The condition of $\Delta_4 = 0$ is termed as **marginal stability** or **indeterminacy**, and we cannot conclude on asymptotic stability.

In the next section, we compute numerically the values of controller gains K_p and K_v where the slow flow equations of the 2R robot driven by PD and model based controllers are asymptotically stable, i.e., the conditions in equation (35) are satisfied. The values and ranges of controller gains where equation (35) results in indeterminacy are computed and, in the next section, we discuss the approach to resolve the indeterminacy.

5 Numerical Results

In this section, we present the numerical results for the asymptotic stability analysis of the 2R planar robot. To perform the numerical study, we choose the physical parameters of an existing robot [16]. These are as given in Table 1.

For purposes of numerical simulation, we use $A_{f_1} = (\pi/2)$ rad, $A_{f_2} = (\pi/4)$ rad and the simulations were performed in MATLAB 2012*Rb* [32] using in-built *ode*45 solver. The relative and absolute tolerances were kept at 10^{-6} and 10^{-9}, respectively and the results were checked for convergence using smaller values of tolerances. The procedure for computing the results shown in this section are as follows:

Table 1. Physical Parameters of the 2-R robot

Parameter	Link 1	Link2
Mass (kg)	20.15	8.25
Length (m)	0.5	0.4
C.G. (m)	0.18	0.26
Inertia (kg – m^2)	6.3	1.64

Following STEP 1 and 2 in the previous section, we compute the values of K_p and K_v at which the slow flow equations given by (27) for the PD controller and equation (28) for the model-based controller are asymptotically stable and the values are plotted in (K_p, K_v) space, also called the chaos map.

In the event that the Routh-Hurwitz condition given by equation (35) yields indeterminacy, we resolve it by computing the Lyapunov exponents [21] of the slow flow equations of the PD and model-based controller. Thus, amongst the indeterminate values and regions, we get chaotic and non-chaotic values and regions. The non-chaotic regions are asymptotically stable. The values for asymptotic stability derived from equation (35) and the chaotic and non-chaotic values are plotted using different markers in the same plots.

To verify whether the controller gains in the chaotic and non-chaotic regions do indeed demonstrate chaos and asymptotic stability respectively, we pick arbitrary values of K_p and K_v in the chaos map in both chaotic and asymptotically stable regions. We then use these (K_p, K_v) values in the original differential equations given by equations (8) and (11) for the PD and model-based controller and compute the Lyapunov exponents for the chosen (K_p, K_v) values. A positive Lyapunov exponent would indicate chaos and the lack of one would indicate asymptotic stability.

We first present the results and observations for the slow flow equations of the PD controller given by equation (27) and then present the same for the slow flow equations of the model-based computed torque controller given by equation (28).

Simulation results for PD control

Fig. (2) represents the plots of controller gains (K_p, K_v) at various values of forcing frequency (Ω). In the figures, the small dots represent asymptotic stability as determined by the Routh-Hurwitz criterion given by equation (35). The small circles represent asymptotically stable regions derived by computing the spectra of Lyapunov exponents at these (K_p, K_v) values in the slow flow equations – at these points the largest Lyapunov exponent is negative. The dark black dots in the plots represent chaotic regions characterized by a largest positive Lyapunov exponent. We can conclude from the plots that the ranges of controller gains (K_p, K_v) for which the 2R robot driven by PD control is asymptotically stable are those regions not represented by the dark black dots.

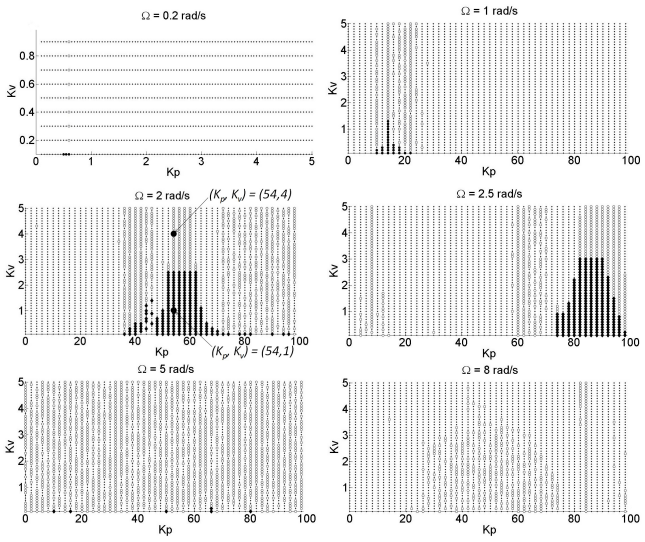

Fig. 2. Chaos maps in (K_p, K_v) space for PD control for various values of forcing frequency Ω

To verify whether the results presented above indeed show asymptotic stability, we pick two arbitrary points in (K_p, K_v) space – one in the chaotic (from the dark black dots) region and one in the asymptotically stable (from the circles and small dots) region as shown in fig. 2b – and compute the Lyapunov exponents. Fig. 3 shows that the largest Lyapunov exponent corresponding to $(K_p, K_v) = (54, 1)$ is positive indicating chaos and absence of asymptotic stability, whereas the largest Lyapunov exponent corresponding to $(K_p, K_v) = (54, 4)$ is negative indicating asymptotic stability. We have performed similar tests for several other points in the regions in the indeterminate and asymptotic stable regions to verify the approach.

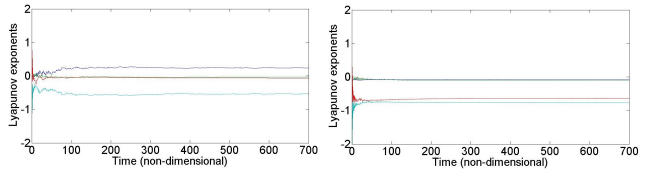

(a) (b)

Fig. 3. Spectra of Lyapunov exponents of the 2R robot equations for PD control – (a) $(K_p, K_v) = (54, 1)$ – chaotic (b) $(K_p, K_v) = (54, 4)$ – asymptotically stable

From the extensive numerical simulation studies, we can make the following observations on the asymptotic stability of 2R planar robot driven by PD control.

For large K_v, the 2R robot is asymptotically stable, irrespective of K_p and the forcing frequency Ω. For low

values of K_p and K_v, the 2R robot is asymptotically stable for higher values of Ω, but is chaotic for lower values of Ω. It can be observed that the range of K_p and K_v values for which the robot is chaotic shifts towards the left with reduction of Ω. For very low Ω (0.2 rad/s), chaos is found near the origin of the chaos map, i.e. at $K_p \approx 0$ and $K_v \approx 0$ (first subfigure in figure 2).

For low values of K_v and high values of K_p, asymptotic stability depends on Ω. For lower values of Ω, for mid-range K_p ($30 < K_p < 75$) and low K_v, the motion of the 2R robot is chaotic. But for high values of K_p ($K_p > 100$), the PD controller is found to be asymptotically stable even for lower values of K_v. For higher values of Ω ($\Omega >= 8$), the PD controller of the 2R robot is asymptotically stable for all values of K_p and K_v.

The results shown are similar to those in the purely numerical studies presented in literature [15, 16]. These results show that the theoretical condition obtained in literature [12] that asymptotic stability exists for positive derivative gains does not take into account possible chaotic motions.

It may be noted that the range of K_p, K_v is kept less than the values for critical damping. The critical damping is given by $K_v = 2\sqrt{K_p}$ and hence, for K_p between 0 to 100, K_v values are from 0 to 20. The values for outside this range was not obtained as it is intuitively well known that over damped systems ($K_v > 2\sqrt{K_p}$) are not chaotic.

Simulation results for model-based control

For slow flow equations of the model-based controller, we present results for an arbitrarily chosen forcing frequency $\Omega = 2$ (rad/s). Results for other Ω similar to the PD control were also done but are not presented.

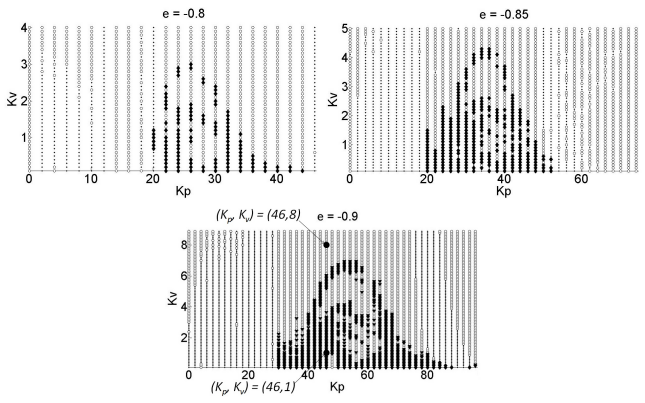

Fig. 4. Chaos maps in (K_p, K_v) space for model-based control for various values of mismatch parameter e

Fig. 4 represents the plots of controller gains (K_p, K_v) at various values of mismatch parameter e. As in the case of PD control, the small dots represent asymptotic stability as determined by the Routh-Hurwitz criterion given by equation (35). The small circles represent asymptotic stability and the dark black dots represent chaos as determined by the computation of Lyapunov exponents in the slow flow equations of the model-based controller. Thus, the dark black dot regions represent chaos whereas the regions given by circles and small dots represent asymptotic stability.

To verify the above results, we again pick two arbitrary points in (K_p, K_v) space – one in the chaotic (dark black dots) region and one in the asymptotically stable (circles and small dots) region as shown in Fig. 4c and substitute these values of controller gains (K_p, K_v) in the original equations of the 2R robot driven by model-based computed torque control (equation (11)). Fig. 5 shows that the largest Lyapunov exponent corresponding to $(K_p, K_v) = (46, 1)$ (in the dark black dot region in the chaos map) is positive indicating chaos, whereas the largest Lyapunov exponent corresponding to $(K_p, K_v) = (46, 8)$ (circles and small dot region in the chaos map) is negative indicating asymptotic stability.

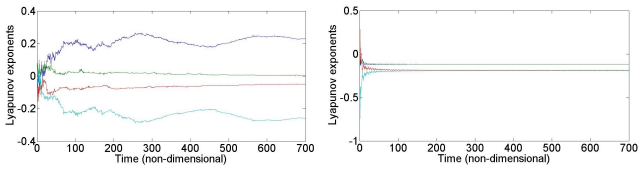

(a) (b)

Fig. 5. Spectra of Lyapunov exponents of the 2R robot equations (11) for model based control – (a) $(K_p, K_v) = (46, 1)$ – chaotic (b) $(K_p, K_v) = (46, 8)$ – asymptotically stable

Observations

From the extensive numerical simulation performed, we make the following observations on the asymptotic stability of 2R planar robot driven by the model-based computed torque control scheme.

Chaos exists for greater underestimation ($e < -0.6$) and is asymptotically stable for $e > -0.6$.

Ranges of K_p and K_v for asymptotic stability vary with the degree of underestimation in the model. For larger underestimation, the ranges of K_p and K_v for asymptotic stability are smaller. For smaller underestimation, the ranges of K_p and K_v for asymptotic stability are larger.

Chaos exists for mid-range to higher values of K_p (depending upon mismatch parameter e) and lower values of K_v. But unlike PD control, chaos exists even for very high values of K_p.

The results shown in this section are similar to those presented in literature [15, 16]. These results, as in the case of PD control, show that the condition obtained in literature [12] that asymptotic stability exists for positive gains, does not take into account the possibility of chaos in the nonlinear dynamical equations representing model based control of a robot.

6 Conclusion

In this paper, the nonlinear dynamical equations of a 2R planar robot driven by PD control and model-based computed torque control following a desired trajectory was analyzed. An semi-analytical method is proposed and the range of controller gains for which the 2R robot is chaotic or asymptotically stable was obtained. The non-dimensional nonlinear ordinary differential equations were analyzed at different time scales by using the method of multiple scales and four slow flow equations were derived. The Routh-Hurwitz criterion was used on the slow flow equations, at a fixed point, to derive analytical conditions for asymptotic stability. The conditions for asymptotic stability were used to compute the ranges of controller gains at which the 2R robot is asymptotically stable or indeterminate. As the use of Routh-Hurwitz criterion can also result in indeterminacy for certain controller gain values, the slow flow equations were further analyzed for the possibility of chaos using Lyapunov exponents. The values of gains, in the indeterminate regions, for which one of the Lyapunov exponent is positive results in chaotic motion and hence for such gain values, the planar 2R robot cannot follow a desired trajectory and be asymptotically stable. The results obtained in this work imply that results related to asymptotic stability of robots following a desired trajectory, available in literature, needs to be re-looked.

The approach of using the method of multiple scales and Routh-Hurwitz criterion is not limited to a planar 2R robot. The number of slow flow equations and the dimension of the Jacobian matrix in n degree-of-freedom robot manipulators would be $2n$ and $2n \times 2n$ respectively. This increase in the number of equations and the dimension of the Jacobian matrix would however make the task of obtaining controller gains for asymptotic stability or chaos more difficult.

References

[1] J. J. E. Slotine and W. Li, 1991, *Applied Nonlinear Control*, Englewood Cliffs, NJ: Prentice Hall, pp. 40-94.

[2] L. Antonio, L. Erjen and N. Henk, 2000, "Global asymptotic stability of robot manipulators with linear PID and PI2D control", *SACTA*, 3(2), pp. 138-149.

[3] K. Rafael, 1995, "A tuning procedure for stable PID control of robot manipulators", *Robotica*, 13(2), pp. 141-148.

[4] A. H. Jose and Y. Wen, 2000, "A high observer-based PD control for robot manipulator", in *Proc. American control Conf.*, Chicago, IL, pp. 2518-2522.

[5] S. S. Ge, T. H. Lee and G. Zu., 1997, "Non-model-based position control of a planar multi-link flexible robot", *Mechanical Systems and Signal Processing*, 11(5), pp. 707-724.

[6] A. K. Amol, L. Gopinathan and R. Goshaidas, 2011, "An adaptive fuzzy controller for trajectory tracking of a robot manipulator", *Intelligent Control and Automation*, 2, pp. 364-370.

[7] Y. Antonio, S. Victor and M. V. Javier, 2011, "Global asymptotic stability of the classical PID controller by considering saturation effects in industrial robots", *International Journal of Advanced Robotic Systems*, 8(4), pp. 34-42.

[8] P. G. Vincente, A. Suguru, H. L. Yun, H. Gerhard and A. Prasad, 2003, "Dynamic sliding PID control for tracking of robot manipulators: Theory and experiments" *IEEE Trans. Robotics and Automation*, 19(6), pp. 967-976.

[9] G. Ruvinda and G. Fathi, 1997, "PD control of closed-chain mechanical systems: An experimental study", in *Proc. of the Fifth IFAC Symposium of Robot Control*, France, pp.79-84.

[10] H. L. Chien, 2007, "Lyapunov based control of a robot and mass spring system undergoing an impact collision", M. S. Thesis, Dept. Mech. and Aero. Eng., Univ. of Florida, Gainesville, FL.

[11] H. Asada and J. J. E. Slotine, 1986 *Robot Analysis and Control*, New York, NJ: John Wiley and Sons, pp. 133-157.

[12] Khalil K. H., 1996, *Nonlinear Systems*, Upper Saddle River, NJ: Prentice Hall, pp. 191-196.

[13] A. A. Burov, 1986, "On the non-existence of a supplementary integral in the problem of a heavy two-link plane pendulum" *Prikl. Matem. Mekhan, USSR*, 50(1), pp.123-125.

[14] P. Yu and Q. Bi, 1988, "Analysis of nonlinear dynamics and bifurcations of a double pendulum", *Jnl. of Sound and Vibration*, 217(4), pp. 691-736.

[15] Lankalapalli S. and Ghosal A., 1996, Possible chaotic motion in a feedback controlled 2R robot, In *Proceedings of the 1996 IEEE International Conference on Robotics and Automation, Minneapolis, MN, April, N. Caplan and T. J. Tarn (eds.)*, IEEE Press, New York, p.p. 1241-1246.

[16] S. Lankapalli and A. Ghosal, 1997, "Chaos in robot control equations", *Intl. Jnl. of Bifurcation and Chaos*, 7(3), pp. 707-729.

[17] K. F. Li, L. Li and Y. Chen, 2002, "Chaotic motion phenomenon in planar 2R robot", *Mech. Sci. and Tech.*, 29(1), pp. 6-8.

[18] R. C. Hilborn, 2000, *Chaos and Nonlinear Dynamics: An Introduction to Scientists and Engineers*, Oxford, New York, NJ, pp. 3-61.

[19] A. H. Nayfeh, 1993, *Introduction to Perturbation Techniques*, New York, NJ: John Wiley and Sons, pp. 388-401.

[20] M. G. O. Arthur, 1999, *Design and Analysis of Control Systems*, Boca Raton, Florida, USA: CRC Press LLC, pp. 323-332.

[21] T. S. Parker and O. S. Chua, 1989, *Practical Numerical Algorithms for Chaotic Systems*, New York, NJ: Springer-Verlag, pp. 57-81.

[22] A. Ghosal, 2006, *Robotics: Fundamental Concepts and Analysis*, New Delhi, India: Oxford Univ. Press, pp. 183-196.

[23] A. S. Ravishankar and A. Ghosal, 1999, "Nonlinear dynamics and chaotic motions in feedback controlled

two and three-degree-of-freedom robots", *Intl. Jnl. of Robotics Res.*, 18(1), pp. 93-108.

[24] A. H. Nayfeh and B. Balachandran, 2004, *Applied Nonlinear Dynamics: Analytical, Computational and Experimental Methods*, Weinheim, Germany: Wiley-VCH Verlag GmbH and Co. KGaA, pp. 108-121.

[25] A. F. El-Bassiouny, 1999, "Response of a three-degree-of-freedom system with cubic nonlinearities to harmonic excitation", *App. Math. and Comp.*, 104, pp. 65-84.

[26] J. Jinchen and C. Yushu, 1999, "Bifurcation in a parametrically excited two degree of freedom nonlinear oscillating system with 1:2 internal resonance", *App. Math. and Mech.*, 20(4), April, pp. 350-359.

[27] B. S. Reddy and A. Ghosal, 2015, "Nonlinear Dynamics of a Rotating Flexible Link", *Journal of Computational and Nonlinear Dynamics, ASME*, 10(6), November, pp. 061015-061015-9.

[28] M. P. Cartmell, S. W. Ziegler, R. Khanin and D. I. M. Forehand, 2003, "Multiple scales analyses of the dynamics of weakly nonlinear mechanical systems", *ASME Appl. Mech. Rev.*, 56(5), September, pp. 455-492.

[29] J. C. Sartorelli and W. Lacarbonara, 2012, "Parametric resonances in a base-excited double pendulum", *Nonlinear Dynamics*, 69, March, pp. 1679-1692.

[30] H. S. Wall, 1945, "Polynomials whose zeros have negative real parts", *The American Mathematical Monthly*, 52(6), pp. 308-322.

[31] P. D. Gupta, N. C. Majee and A. B. Roy, 2008, "Asymptotic stability, orbital stability of Hopf-bifurcating periodic solution of a simple three-neuron artificial neural network with distributed delay", *Nonlinear Analysis: Mod. and Control*, 13(1), pp. 9-30.

[32] *Matlab Version 8.0 (R2012Rb)*, Mathworks Inc., Natick, MA, 2012.

Appendix

Terms in (17)

In (17), the values of $\omega_i,\ i = 1,2$ are given by

$$\omega_i = \sqrt{1/2L_{q3}(K_{pn}(L_{q2} \pm \sqrt{L_{q1}}))}$$

where

$L_{q2} = 2 + P_1 + P_2 + 2P_2P_3,\ L_{q3} = P_1 + P_2 - P_2^2P_3^2$

$L_{q1} = 4 + 4P_2P_3(P_1 + 2) + (P_1 + P_2)^2 + 4P_2^2P_3(1 + 2P_3)$

Terms in (24, 25)

$J_{12k} = (1/\omega_1 L_{11})L_{12k},\ J_{22k} = (1/\omega_2 l_{21})L_{22k},\ k = 1,..,4,$

$J_{1k} = (1/\omega_1 L_{11})L_{1k}\ k = 3,4,\ J_{23} = (1/\omega_2 L_{21})L_{23}$

$L_{1j} = R_{1j}(K_{pn} - \omega_1^2) + R_{2j}(1 + P_2P_3)\omega_1^2 \quad \forall i = 1,3,4$

$L_{12j} = R_{12j}(K_{pn} - \omega_1^2) + R_{22j}(1 + P_2P_3)\omega_1^2\ \forall i = 1,..,4$

$L_{2j} = S_{2j}(K_{pn} - \omega_2^2) + S_{2j}(1 + P_2P_3)\omega_2^2 \quad \forall i = 1,3$

$L_{22j} = S_{12j}(K_{pn} - \omega_2^2) + S_{22j}(1 + P_2P_3)\omega_2^2\ \forall i = 1,..,4$

where $R_{11} = -2(P_1 + 1 + P_2(1 + 2P_3) + (1 + P_2P_3)c_{21})$

$R_{122} = -P_2P_3F_2^2\omega_1^2(2 + c_{21})(E_2^2 + E_1^2), R_{121} = -K_{vn}\omega_1$

$R_{124} = -P_2P_3c_{22}^2\omega_1^2(2 + c_{21}),\ R_{221} = -K_{vn}\omega_1 c_{21},$

$R_{123} = (1/2)(-P_2P_3c_{21}^2\omega_1^2(2 + c_{21})),$

$S_{121} = -K_{vn}\omega_2,\ S_{21} = -2(1 + P_2P_3 + c_{22})$

$R_{13} = -P_2P_3(\omega_2 + 2)(\frac{F_2^2(2 + c_{22})\omega_2}{2} + c_{22}F_2(2F_1 + F_2)),$

$R_{21} = -2(1 + P_2P_3 + c_{21})$

$R_{14} = (1/2)(-3P_2P_3F_2^2(2F_1 + F_2)),\ S_{221} = -K_{vn}\omega_2 c_{22}$

$S_{11} = -2(P_1 + 1 + P_2(1 + 2P_3) + (1 + P_2P_3)c_{22})$

$S_{13} = P_2P_3(\omega_1 - 2)(\frac{-F_2^2(2 + c_{21})\omega_1}{2} + c_{21}F_2(2F_1 + F_2))$

$S_{122} = -P_2P_3F_2^2\omega_2^2(2 + c_{22})(E_2^2 + E_1^2)$

$S_{123} = -P_2P_3c_{21}^2\omega_2^2(2 + c_{22}),$

$R_{223} = (1/2)(-P_2P_3c_{21}\omega_1^2(2 + 3c_{21}))$

$R_{224} = -P_2P_3(c_{21}\omega_2^2(2 + c_{22}) + c_{22}(c_{21}\omega_2^2 + c_{22}\omega_1^2)),$

$R_{24} = (1/2)(-P_2P_3F_1F_2(2F_1 - F_2))$

$R_{222} = -P_2P_3(E_2^2 + E_1^2)(c_{21}F_1(2F_1 + F_2) + F_2(c_{21}F_1 + F_2\omega_1^2)),$

$R_{23} = P_2P_3(\frac{F_1c_{22}(2F_1 - F_2)}{2} + F_2(2F_1\omega_2 - \frac{c_{22}F_1 + F_2\omega_2^2}{2})),$

$S_{224} = -(1/2)(P_2P_3c_{22}\omega_2^2(2 + 3c_{22}))$

$S_{222} = -P_2P_3(E_2^2 + E_1^2)(c_{22}F_1(2F_1 + F_2) + F_2(c_{22}F_1 + F_2\omega_2^2)),$

$S_{223} = -P_2P_3(c_{22}\omega_1^2(2 + c_{21}) + c_{21}(c_{21}\omega_2^2 + c_{22}\omega_1^2)),$

$S_{23} = P_2P_3(\frac{F_1c_{21}(2F_1 - F_2)}{2} - F_2(2F_1\omega_1 + \frac{c_{21}F_1 + F_2\omega_1^2}{2})),$

$S_{124} = -(1/2)(P_2P_3c_{22}^2\omega_2^2(2 + c_{22}))$

where $F_1 = \dfrac{(K_{pn} - 1)A_{f_1} + (1 + P_2P_3)A_{f_2}}{E_f},$

$F_2 = \dfrac{(1 + P_2P_3)A_{f_1} + (K_{pn} - P_1 - 1 - P_2 - 2P_2P_3)A_{f_2}}{E_f}$

$E_f = (K_{pn} - 1)(K_{pn} - (P_1 + 1 + P_2 + 2P_2P_3)) -$

$(1 + P_2P_3)^2, c_{21} = \dfrac{K_{pn} - \omega_1^2}{(1 + P_2P_3)\omega_1^2}, c_{22} = \dfrac{K_{pn} - \omega_2^2}{(1 + P_2P_3)\omega_2^2}$

Terms in equation (28)

Considering the following terms

$$D_{11} = K_{pn}\alpha_3 - \omega_1^2, \quad D_{21} = K_{pn}\alpha_3 - \omega_2^2$$
$$D_{12} = (1+P_2P_3)\omega_1^2 - K_{pn}(\alpha_3+\alpha_2), E_1 = \frac{1-K_{pn}}{2}$$
$$D_{22} = (1+P_2P_3)\omega_2^2 - K_{pn}(\alpha_3+\alpha_2), E_2 = \frac{K_{vn}}{2}$$

we have

$$J_{a1} = 2J_{13}E_1E_2 - J_{15}E_2,\ J_{a2} = J_{13}(E_2^2 - E_1^2) + J_{15}E_1,$$
$$J_{a3} = J_{14}E_1(3E_2^2 - E_1^2) - J_{16}(E_2^2 - E_1^2)$$
$$J_{a4} = J_{14}E_2(E_2^2 - 3E_1^2) + 2J_{16}E_1E_2,\ J_{a5} = 2J_{23}E_1E_2$$
$$-J_{25}E_2,\ J_{a6} = J_{23}(E_2^2 - E_1^2) + J_{25}E_1$$
$$J_{12k} = \frac{L_{12k}}{\omega_1 L_{11}}\ \forall k = 1-4,\ J_{1k} = \frac{L_{1k}}{\omega_1 L_{11}}\ \ \forall k = 3-6$$
$$J_{22k} = \frac{L_{22k}}{\omega_2 L_{21}}\ \forall k = 1-4,\ J_{2k} = \frac{L_{2k}}{\omega_2 L_{21}}\ \ \forall k = 3,5$$
where $L_{1k} = Q_{1k}D_{11} + Q_{2k}D_{12}\ \ \forall k = 1,3,4,5,6$
$$L_{2k} = R_{1k}D_{21} + R_{2k}D_{22}\ \ \forall k = 1,3,5$$
$$L_{12k} = Q_{12k}D_{11} + Q_{22k}D_{12} \qquad \forall k = 1,2,3,4$$
$$L_{22k} = R_{12k}D_{21} + R_{22k}D_{22} \qquad \forall k = 1,2,3,4$$
where $Q_{11} = -2(P_1 + 1 + P_2(1+2P_3) + C_{21}(1+P_2P_3))$
$Q_{15} = \alpha_2(2A_{f_1} + A_{f_2})E_1C_{22}F_2, R_{121} = -K_{vn}\omega_2(\alpha_1 +$
$(2+C_{22})\alpha_2 + C_{22}\alpha_3), Q_{121} = -K_{vn}\omega_1(\alpha_1 +$
$(2+C_{21})\alpha_2 + C_{21}\alpha_3), Q_{16} = \alpha_2(2A_{f_1} + A_{f_2})E_1\frac{F_2^2}{2}$
$$Q_{14} = F_2^2(2F_1+F_2)\left(\frac{\alpha_2(2+K_{pn}) - 3P_2P_3}{2}\right)$$
$Q_{122} = (E_2^2 + E_1^2)(P_2P_3(-F_2^2\omega_1^2(2+C_{21}) - 2C_{21}F_2(2F_1$
$+F_2)) + (P_2P_3 - \alpha_2)(2C_{21}F_2(2F_1+F_2))) - 2\alpha_2C_{21}$
$E_1^2F_2(2A_{f_1} + A_{f_2}) + K_{pn}\alpha_2(2F_2^2(2+C_{21}) + 4C_{21}F_2$
$(2F_1+F_2))\left(\frac{E_2^2+E_1^2}{2}\right), Q_{123} = (P_2P_3 - \alpha_2)C_{21}^2\omega_1^2$
$(2+C_{21}) + P_2P_3\left(\frac{-3C_{21}^2\omega_1^2(2+C_{21})}{2}\right) + K_{pn}\alpha_2$
$\left(\frac{3C_{21}^2(2+C_{21})}{2}\right), R_{15} = \alpha_2(2A_{f_1} + A_{f_2})E_1C_{21}F_2$
$Q_{124} = -P_2P_3C_{22}^2\omega_1^2(2+C_{21}) - 2\alpha_2C_{21}C_{22}\omega_2^2(2+C_{22})$
$+ K_{pn}\alpha_2\left(\frac{2C_{22}^2(2+C_{21}) + 4C_{21}C_{22}(2+C_{22})}{2}\right), Q_{15} =$
$\alpha_2(2A_{f_1} + A_{f_2})E_1C_{22}F_2, R_{11} = -2(P_1 + 1 + P_2(1+$
$2P_3) + C_{22}(1+P_2P_3)), R_{122} = (E_2^2 + E_1^2)(P_2P_3(-F_2^2\omega_2^2$
$(2+C_{22}) - 2C_{22}F_2(2F_1+F_2)) + (P_2P_3 - \alpha_2)(2C_{22}F_2$
$(2F_1+F_2))) - 2\alpha_2C_{22}E_1^2F_2(2A_{f_1} + A_{f_2}) +$
$K_{pn}\alpha_2(2F_2^2(2+C_{22}) + 4C_{22}F_2(2F_1+F_2))\left(\frac{E_2^2+E_1^2}{2}\right)$
$$R_{124} = P_2P_3\left(\frac{-3C_{22}^2\omega_2^2(2+C_{22})}{2}\right) + (P_2P_3 - \alpha_2)$$
$(C_{22}^2\omega_2^2(2+C_{22})) + K_{pn}\alpha_2(\frac{3C_{22}^2(2+C_{22})}{2}), R_{123} = -P_2$
$P_3C_{21}^2\omega_2^2(2+C_{22}) - 2\alpha_2C_{21}C_{22}\omega_1^2(2+C_{21}) + K_{pn}\alpha_2$
$\left(\frac{2C_{21}^2(2+C_{22}) + 4C_{21}C_{22}(2+C_{21})}{2}\right)$
$$R_{21} = -2(1+P_2P_3+C_{22}),\ Q_{21} = -2(1+P_2P_3+C_{21})$$
$$Q_{13} = -P_2P_3\left(\frac{F_2^2\omega_2^2(2+C_{22})}{2} + C_{22}F_2(2F_1+F_2)\right) +$$
$$K_{pn}\alpha_2F_2\left(\frac{F_2(2+C_{22}) + 2C_{22}(2F_1+F_2)}{2}\right) -$$
$(P_2P_3 - \alpha_2)(F_2^2\omega_2(2+C_{22}) + (\omega_2+1)C_{22}F_2(2F_1+F_2))$
$$Q_{26} = \alpha_2A_{f_1}E_1\frac{F_2^2}{2},\ R_{221} = -K_{vn}\omega_2(\alpha_3 + \alpha_2 + C_{22}\alpha_3)$$
$Q_{25} = \alpha_2A_{f_1}E_1C_{22}F_2, R_{25} = \alpha_2A_{f_1}E_1C_{21}F_2, Q_{221} =$
$-K_{vn}\omega_1(\alpha_3 + \alpha_2 + C_{21}\alpha_3)$
$$R_{13} = -P_2P_3\left(\frac{F_2^2\omega_1^2(2+C_{21})}{2} + C_{21}F_2(2F_1+F_2)\right) +$$
$$K_{pn}\alpha_2F_2\left(\frac{F_2(2+C_{21}) + 2C_{21}(2F_1+F_2)}{2}\right) +$$
$(P_2P_3 - \alpha_2)(F_2^2\omega_1(2+C_{21}) + (\omega_1-1)C_{21}F_2(2F_1+F_2))$
$$Q_{223} = (\alpha_2 - P_2P_3)C_{21}\omega_1^2 - 3P_2P_3C_{21}^2\frac{\omega_1^2}{2} + 3K_{pn}\alpha_2\frac{C_{21}^2}{2}$$
$Q_{222} = -2\alpha_2C_{21}E_1^2F_2A_{f1} + (E_2^2 + E_1^2)(2(\alpha_2 - P_2P_3)$
$C_{21}F_1^2 - P_2P_3(F_2^2\omega_1^2 - 2C_{21}F_1F_2) + \frac{K_{pn}\alpha_2}{2}(2F_2^2 +$
$4C_{21}F_1F_2)), R_{222} = -2\alpha_2C_{22}E_1^2F_2A_{f_1} +$

$$(E_2^2+E_1^2)(\frac{K_{pn}\alpha_2}{2}(2F_2^2+4C_{22}F_1F_2)-P_2P_3(F_2^2\omega_2^2-$$
$$2C_{22}F_1F_2)+2(\alpha_2-P_2P_3)C_{22}F_1^2)$$
$$R_{224}=(\alpha_2-P_2P_3)C_{22}\omega_2^2-3P_2P_3C_{22}^2\frac{\omega_2^2}{2}+3K_{pn}\alpha_2\frac{C_{22}^2}{2}$$
$$Q_{24}=\frac{F_1F_2}{2}(F_1(P_2P_3-2\alpha_2)+F_2K_{pn}\alpha_2), Q_{224}=$$
$$K_{pn}\alpha_2C_{22}(C_{22}+2C_{21})-P_2P_3(C_{22}^2\omega_1^2+2C_{21}C_{22}$$
$$\omega_2^2)-2(\alpha_2-P_2P_3)C_{21}\omega_2^2, R_{223}=K_{pn}\alpha_2C_{21}(C_{21}+2$$
$$C_{22})-P_2P_3(C_{21}^2\omega_2^2+2C_{21}C_{22}\omega_1^2)-2(\alpha_2-P_2P_3)C_{22}\omega_1^2$$

where

$$\omega_1=\sqrt{\frac{K_{pn}(L_{q1}+\sqrt{L_{q2}})}{L_{q3}}}, \omega_2=\sqrt{\frac{K_{pn}(L_{q1}-\sqrt{L_{q2}})}{L_{q3}}}$$
$$\text{where}\quad L_{q1}=\alpha_1+\alpha_3(P_1+P_2-1)-2P_2P_3\alpha_2,$$
$$L_{q2}=P_1^2\alpha_3^2 4P_1P_2P_3\alpha_2\alpha_3-2P_1P_2\alpha_3^2-2P_1\alpha_1\alpha_3+$$
$$4P_2^2P_3^2\alpha_1\alpha_3-4P_2^2P_3^2\alpha_3^2-4P_2^2P_3\alpha_2\alpha_3+4P_1\alpha_2^2+$$
$$P_2^2\alpha_3^2+4P_2P_3\alpha_2(\alpha_3-\alpha_1)-2P_2\alpha_1\alpha_3+4P_2\alpha_2^2+2P_2\alpha_3^2$$
$$+\alpha_1^2-2\alpha_1\alpha_3+\alpha_3^2, L_{q3}=P_1+P_2-P_2^2P_3^2+2P_1\alpha_3^2$$
$$C_{21}=\frac{\omega_1^2(1+P_2P_3)-K_{pn}(\alpha_3+\alpha_2)}{(K_{pn}\alpha_3-\omega_1^2)},$$
$$C_{22}=\frac{\omega_2^2(1+P_2P_3)-K_{pn}(\alpha_3+\alpha_2)}{(K_{pn}\alpha_3-\omega_2^2)}$$
$$F_1=\frac{1}{E_f}((K_{pn}\alpha_3-1)(A_{f_1}\alpha_1+A_{f_2}\alpha_3+\alpha_2(2A_{f_1}+A_{f_2}))$$
$$+(1+P_2P_3-K_{pn}(\alpha_3+\alpha_2))(A_{f_1}(\alpha_3+\alpha_2)+A_{f_2}\alpha_3))$$
$$F_2=\frac{1}{E_f}((1+P_2P_3-K_{pn}(\alpha_3+\alpha_2))(A_{f_1}\alpha_1+A_{f_2}\alpha_3+$$
$$\alpha_2(2A_{f1}+A_{f2}))+(K_{pn}(\alpha_1+2\alpha_2)-(P_1+1+P_2+$$
$$2P_2P_3))(A_{f_1}(\alpha_3+\alpha_2)+A_{f_2}\alpha_3))$$

where

$$E_f=(K_{pn}\alpha_3-1)(K_{pn}(\alpha_1+2\alpha_2)-$$
$$(P_1+1+P_2+2P_2P_3))-(1+P_2P_3-K_{pn}(\alpha_3+\alpha_2))^2$$

Non-dimensional parameters K_{pn} and K_{vn} are

$$K_{pn}=\frac{K_p}{\Omega^2},\qquad K_{vn}=\frac{K_v}{\Omega}$$

List of Table Captions

Table 1: Physical Parameters of the 2-R robot

List of Figures Captions

Figure 1: A planar 2R robot

Figure 2: Chaos maps in (K_p,K_v) space for PD control for various values of forcing frequency Ω

Figure 3: Spectra of Lyapunov exponents of the 2R robot equations for PD control – (a) $(K_p,K_v)=(54,1)$ – chaotic (b) $(K_p,K_v)=(54,4)$ – asymptotically stable

Figure 4: Chaos maps in (K_p,K_v) space for model-based control for various values of mismatch parameter e

Figure 5: Spectra of Lyapunov exponents of the 2R robot equations (11) for model based control – (a) $(K_p,K_v)=(46,1)$ – chaotic (b) $(K_p,K_v)=(46,8)$ – asymptotically stable